Synthesis and performance of $La_{0.5}Sr_{0.5}CoO_3$ cathode for low and intermediate temperature solid oxide fuel cells

Baijnath, Pankaj Kumar Tiwari, Suddhasatwa Basu*

Department of Chemical Engineering, Indian Institute of Technology Delhi, New Delhi 110016, India

*Corresponding author

DOI: 10.5185/amp.2018/895
www.vbripress.com/amp

Abstract

In the present work, different synthesis methods i.e., sol-gel method, glycine-nitrate method and solid state route have been used to synthesize lanthanum strontium cobaltite (LSCO), which is utilized as cathode in low and intermediate temperature solid oxide fuel cell (SOFC). Calcination temperature for LSCO has been determined by TGA. XRD, SEM, EDX and TEM have been used to assess the phase purity, crystallite size, morphology, distribution of constituent elements and particle size of synthesized LSCO material. Two-probe AC conductivity method has been used to calculate the ionic conductivity of LSCO in air environment between 400-800°C. LSCO synthesized by sol-gel method provided highest ionic conductivity of 0.42 S/cm at 700°C and lowest activation energy of 31.60 kJ/mol between 500 to 700 °C among all the methods. LSCO synthesized by sol-gel method gives lowest area specific resistance (ASR) of 3.52 Ω cm^2 at 800°C for half-cell (LSCO/YDC). High ionic conductivity and low polarization resistance established LSCO synthesized by sol-gel method, as the potential cathode material.

Keywords: SOFC; LSCO; cathode material; method of preparation; area specific resistance.

Introduction

The electrochemical reduction of oxygen takes place at cathode in solid oxide fuel cell (SOFC) [1]. Cathode must have high electrochemical activity and electrical conductivity and should be stable under oxidizing conditions and maintain sufficient porosity at the operating temperature. It must have a comparable thermal expansion coefficient and chemical compatibility with the electrolyte and interconnect materials [1-3]. Oxygen reduction reaction (ORR) takes place at the cathode close to triple phase boundaries (TPBs), where oxygen ion conductor, electronic conductor, and gas phase come in contact [1,4].

Lanthanum strontium manganite (LSM) has been used as cathode material in conventional SOFC. LSM shows poor ionic conductivity at ambient oxygen partial pressure. During high temperature sintering LSM react with yittria stabilized zirconia (YSZ) and forms insulating lanthanum zirconate ($La_2Zr_2O_7$) and strontium zirconate ($SrZrO_3$) at the electrode and electrolyte interface. The insulating phases between LSM and YSZ induce high ohmic loss and polarization loss. The losses have large impact on performance of SOFCs and should be as minimum as possible. Formation of lanthanum zirconate will be high when (La+Sr) content at the A-site is greater than Mn^{3+} ions at the B-site and when Sr/La ratio is less than 0.43. High Sr content leads to Sr depletion from the lattice and eventual $SrZrO_3$ formation [5-7].

To increase the efficiency of SOFCs at low and intermediate temperature, mixed ionic and electronic conductors (MIECs) are used as cathode material. MIECs shows both properties of ionic and electronic conductivities. MIECs are ABO_3-type perovskite, where A belongs to rare earth ions (e.g., La) and B belongs to the transition metal ions (e.g., Co) and A-site is doped with other earth metal. MIEC, strontium doped lanthanum cobaltite ($La_{1-x}Sr_xCoO_{3-\delta}$ - LSCO) reduces the losses and enhances the performance of cells. Here strontium is doped on lanthanum. At low current density LSCO shows linear i-V characteristics and at high current density, it follows Tafel kinetics [8-11]. High chemical diffusion coefficient of oxygen in LSCO helps in bulk transport of oxygen, which leaves larger region of the electrode for ORR that enhance the performance of SOFC [12]. Due to octahedral symmetry around the transition metal at high temperature metallic or semiconducting band structure provide high electronic conduction [13]. At operating conditions, MIECs support large number of oxygen ion vacancies which enhance significantly bulk ionic oxygen transport [4, 14].

Sr-doped lanthanum cobaltites are p-type conductors due its high electrical conductivity. Conductivity increases with increase in temperature, increase in oxygen partial pressure and decrease in Sr-content [15, 16]. Cobalt content ensures good electronic conductivity and a slight oxygen over-stoichiometry favours the oxygen transport

and also enhances electrochemical properties. Metal-oxygen distance shortening with increase in Sr-content increases the surface area [17, 18]. Surface area is an important factor for reaction rate on LSCO electrode. High performance electrodes can be obtained by using MIEC electrode with a large surface area. For the MIEC cathodes, the role of surface area in improving their performance lies in the fact that a higher surface area leads to more active sites for the oxygen reduction reaction. LSCO electrode synthesized by tape casting and laser ablation method provides high surface area for reaction [19, 20]. It is reported that $La_{0.6}Sr_{0.4}CoO_{3-\delta}$ cathode material synthesized using citric acid (CA) and ethylenediaminetetraacetic acid (EDTA) complexing method and calcined at 1000 °C shows cubic perovskite structure [21]. Polarization resistance reduced in air for symmetric LSCO cathode on a GDC electrolyte substrate [22]. Egger et al. synthesized $La_{0.5}Sr_{0.5}CoO_{3-\delta}$ and $La_{0.6}Sr_{0.4}CoO_{3-\delta}$ cathode materials for IT-SOFCs by modified Pechini process and characterized by the conductivity relaxation technique between 525°C-725°C at oxygen partial pressures of 0.1, 0.01 and 0.001 bar. They reported ionic conductivity of 1×10^{-2} S/cm with an activation energy of 118 kJ/mol for $La_{0.5}Sr_{0.5}CoO_{3-\delta}$ at 725°C [15]. Hu et al. synthesized $La_{2-x}Sr_xCoO_{4-\delta}$ (x=0.9, 1.0 and 1.1) using a microwave assisted citrate-nitrate combustion method [16]. Electrochemical performance is improved by varying LSCO and cerium gadolinium oxide (CGO) ratio (50 wt% LSCO-50 wt% CGO) [17].

There is scarcity of literature to provide comparative studies of LSCO cathode synthesis by different methods. It is seen that the different synthesis methods of LSCO provide different conductivities and ASR values. In the present work, $La_{0.5}Sr_{0.5}CoO_3$ (LSCO) has been synthesized by three different synthesis routes i.e., sol-gel, glycine-nitrate and solid state route. Comparative study has been done for ionic conductivity and performance of SOFC half-cell. Two-probe AC conductivity method (Electrochemical Impedance Spectra, EIS) has been used to evaluate ionic conductivity of LSCO. To study the cathode polarization resistance, $La_{0.5}Sr_{0.5}CoO_3$/Yttria doped ceria (YDC) half-cells are measured.

Experimental

Materials and methods

For the synthesis of LSCO powder, $La(NO_3)_3.6H_2O$ (99.9% Alfa Aesar, USA), $Sr(NO_3)_2$ (99.9% Alfa Aesar, USA) and $Co(NO_3)_2.6H_2O$ (97.7% Alfa Aesar, USA) were used as precursors in all the synthesis methods.

In sol-gel method, precursors in stoichiometric ratio were dissolved in distilled water. Citric acid ($C_6H_8O_7$) (anhydrous pure, Merck, India) was dissolved in distilled water in a separate container. Both the solutions were mixed in a 1 litre glass beaker, under constant stirring condition on a hot plate to evaporate the excess water. The temperature of hot plate was kept at 80 °C for 3 h. The gel was obtained after heat treatment at 100 °C for 1 h and at 120 °C for 2 h. Further it was calcined at 800 °C for 2 h and at 850 °C for 10 h to get perovskite LSCO powder.

In glycine-nitrate method, precursors in stoichiometric ratio were dissolved in distilled water. The solution was mixed in a 1 litre glass beaker, under constant stirring condition on a hot plate to evaporate the excess water. The temperature of the hot plate was kept at 100 °C for 1 h. After significant reduction of the solution volume, the glycine ($C_2H_5NO_2$) (purified, Merck, India) dissolved in distilled water was added to it. The amount of glycine used was calculated in order to obtain a glycine-nitrate molar ratio of 2:1. The self-combustion of glycine/nitrate starts at 200 °C. The obtained powder was calcined at 800 °C for 2 h and at 850 °C for 10 h to get perovskite LSCO powder. Effect of fuel on crystallite size was analyzed using glycine nitrate method by varying glycine to nitrate ratio (g/n ratio) and keeping other parameters, calcination temperature and time constant. Glycine and nitrate were taken in three different ratios, i.e. g/n=0.5:1, 1:1 and 2:1.

In solid state reaction, precursors in stoichiometric ratio were mixed thoroughly in an automatic agate mortar and pestle for 4 h. This powder was sintered at 1250 °C to get perovskite LSCO powder. **Fig. 1** compares flowchart of synthesis process for sol-gel, glycine nitrate and solid state route to obtain perovskite, LSCO powder and sintered pellets.

Thermal analysis of samples was analyzed using NETZSCH TG 209 F3 Tarsus between temperature range 28-900 ºC with heating rate of 10 ºC/min, which provide information about calcination temperature. X-ray diffraction (XRD) was carried out to assess phase purity and crystallite size of cathode powder and cathode pellet. Rigaku MiniFlex X-ray diffractometer with Cu Kα radiation (wavelength, λ=1.54 Å) was used for this purpose. The 2θ range was set from 20-80º with a step size of 4º/min. Average crystallite size of synthesized LSCO cathode was calculated using Scherrer's equation:

$$d = \frac{K\lambda}{\beta \cos\theta}$$

where, d is the crystallite size, K is Scherrer constant (0.94), λ is the wavelength of radiation (1.54), β is the full width at half maximum (FWHM) in radians and θ is the Bragg angle. Scanning electron microscopy (SEM) and energy-dispersive X-ray spectroscopy (EDX) for LSCO powder, LSCO pellet and composite half-cell were carried out for microstructure and elemental analysis using JEOL JSM 6010 LA JAPAN. The microstructure analysis was carried before and after cell testing to ascertain the changes occurring during the operation. The particle size analyses of the cathodes were carried out by transmission electron microscope (TEM CM 12, Phillips).

To fabricate cathode pellet, the weighed amount of LSCO powder was placed in a clean die and the uniaxially pressed into pellets of 15 mm diameter by applying 150 kg/cm^2 pressure. Pellets were sintered at 1250 °C for 12 h. Cathode pellets of LSCO powder were used to evaluate the electrochemical performance between temperature range 400-800 ºC in a split furnace.

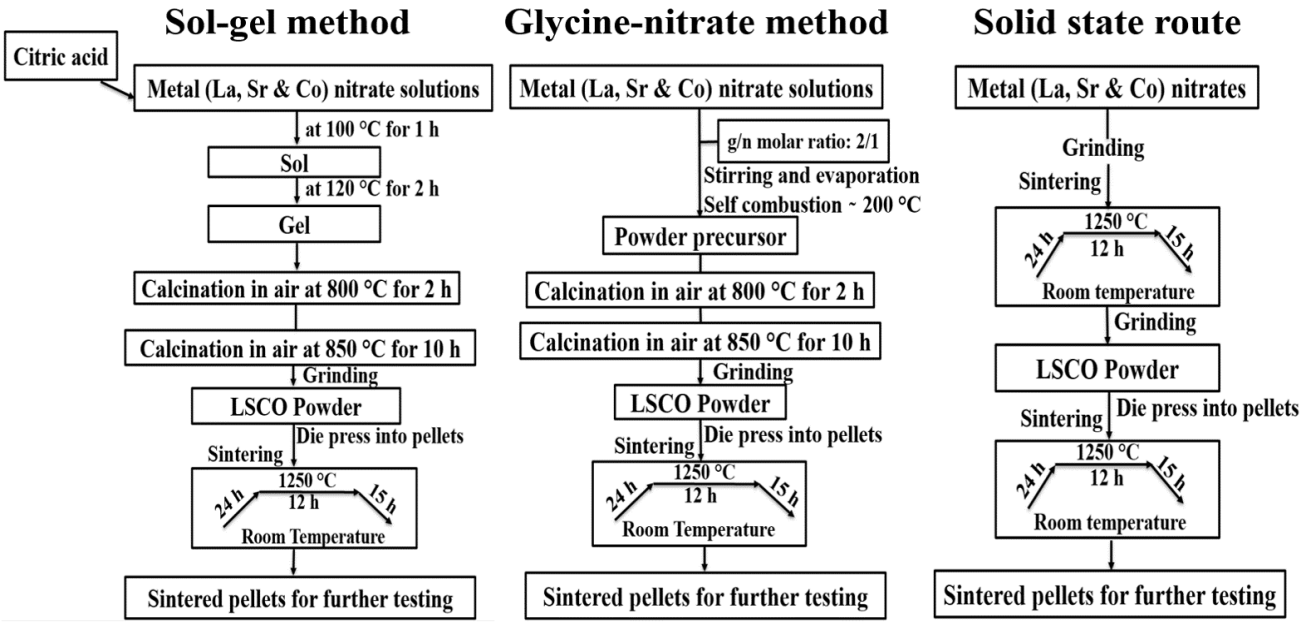

Fig. 1. Flowchart of the sol-gel, glycine-nitrate and solid state route for LSCO perovskite synthesis.

Potentiostat/Galvanostat (PGSTAT 302N Autolab) was used to carry out electrochemical impedance spectra between frequency range 1 MHz to 0.1 Hz. To calculate the ionic conductivity, the following formula is being used:

$$\sigma = \frac{L}{RA}$$

where, σ is the conductivity, L is the thickness of pellet, R is the resistance and A is active area.

For half-cell fabrication, yttria doped ceria (YDC) powder (99.9% American Elements, USA) was used as electrolyte. A 5 wt% solution of polyvinyl alcohol (PVA) (Fisher Scientific, India) was used as binder and starch (Merck, India) as pore former. To fabricate composite cathode, LSCO (70 wt%), electrolyte YDC (30 wt%) and starch (30 wt% of total LSCO and YDC) were mixed thoroughly in an automatic agate mortar and few drops of PVA solution were added and mixed thoroughly to make slurry. The slurry was dried in an oven at 100°C. The solid mixture was crushed to very fine powder using an automatic agate mortar for 4-5 h. Composite cathode (LSCO:YDC=70:30) and electrolyte (YDC) were co-pressed into half cells of 15 mm diameter by applying 150 kg/cm^2 pressure. The silver wires were attached on both side of cathode pellets and half-cells using silver conductive ink and analyzed between 400-800 ºC in a split furnace. Potentiostat/Galvanostat (PGSTAT 302N Autolab) was used to carry out electrochemical impedance spectra for half-cell between frequency 1 MHz - 0.1 Hz. The real part of the impedance was plotted on the x-axis and the negative of the imaginary part of the impedance was plotted on the y-axis (Nyquist plot). The high frequency intercept on the x-axis gives the ohmic resistance of the cell which is due to the electrolyte. The diameters of the semicircles are a measure of the polarization resistances of the electrodes.

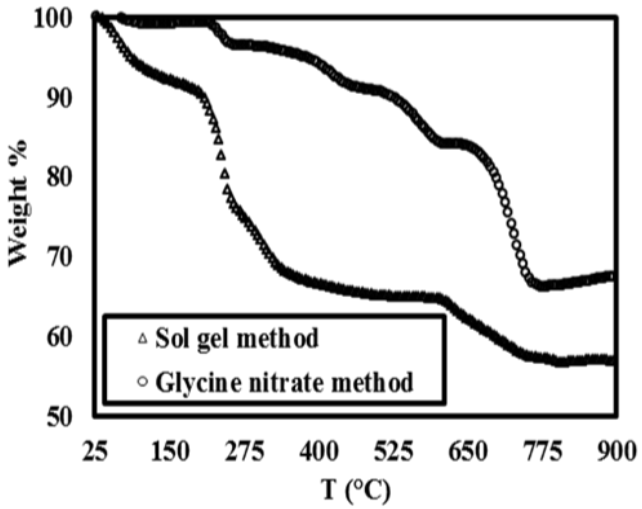

Fig. 2. TGA curve of LSCO cathode material as synthesized by (a) sol-gel method, and (b) glycine-nitrate method.

Results and discussion

Thermogravimetric analysis (TGA) has been done to determine calcination temperature of synthesized LSCO powder to obtain phase pure perovskite structure. **Fig. 2** shows the TGA curve between temperature 28-900 ºC for LSCO cathode synthesized by sol-gel method and glycine-nitrate method. It has been observed from TGA curve of sol-gel method that decrease in weight loss starts at temperature 28 ºC, which may be due to formation of some gaseous product escaping from the sample. Evaporation of remaining water, low boiling temperature organic species and decomposition of nitrates occurs between temperature range 28-215ºC. Boiling

point of citric acid and glycine is 175ºC and 205ºC, respectively. Volatilization of organic species and decomposition of residual nitrates occurs between 215 to 608 ºC. It has been reported that oxygen vacancies also contributed in weight loss around 350ºC. The weight loss observed between 608 to 760ºC might be initiated from the removal of residual or trapped carbon which is formed as intermediate products [21]. There is no weight loss after 760ºC in case of LSCO cathode synthesized by sol-gel method, whereas small weight gain is observed around 780 ºC in TGA curve of LSCO synthesized by glycine nitrate method. From the above observation, one may conclude that the calcination temperature required to get LSCO perovskite phase is between 800-850ºC. For the cathode synthesized by solid state route all the precursors have been mixed and kept at 1250 ºC to form solid solution of LSCO. In this case it is not required to determine the calcination temperature.

The nanoparticles of LSCO cathode powder are investigated to assess phase purity using XRD analysis. Data from Joint Committee on Powder Diffraction Standards-International Centre for Diffraction Data (JCPDS) has been used for phase identification. **Fig. 3 (a)** shows the XRD patterns of LSCO powder as synthesized by different methods. The observed major peaks of cathode powder are matched with JCPDS card no. 48-0122 and confirms the formation of perovskite phase of LSCO powder. Some small peaks correspond to strontium oxide (JCPDS card no. 49-0692) at 48º and cobalt oxide (JCPDS Card No. 43-1004) at 61º have been also detected. Effect of fuel on crystallite size has been analyzed using glycine nitrate method by varying glycine to nitrate ratio (g/n ratio) and keeping other parameters like calcination temperature and time constant. XRD patterns shown in **Fig. 3 (b)** confirms the perovskite phase of LSCO powder correspond to different g/n ratios. Average crystallite size of synthesized LSCO powder for different g/n ratios is calculated using Scherrer's equation. Average crystallite size is decreased as glycine amount increased. It is observed that g/n=2:1 provides smallest crystallite size (21.9 nm). Average crystallite size have been presented in **Table 1**. Some extra peaks with very less intensity are detected for g/n=0.5:1 and 1:1 at 25º, 29º and 43º but there is no extra peak observed for g/n=2:1. It can be infer from the observed XRD patterns that fuel rich environment provides phase pure LSCO perovskite.

Table 1. Crystallite size for different glycine and nitrate ratio.

Glycine nitrate method		
S. No	Glycine:Nitrate	Crystallite Size (nm)
1.	0.5:1	30.4
2.	1:1	23.2
3.	2:1	21.9

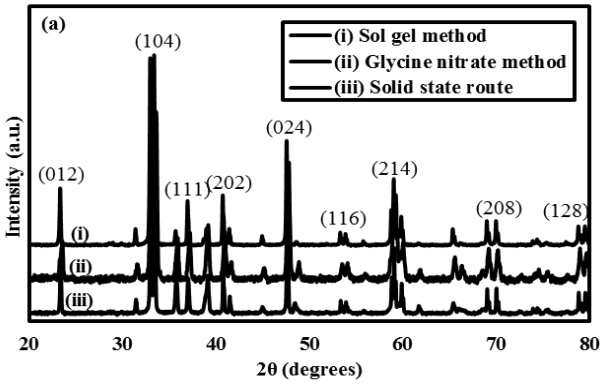

Fig. 3. (a) XRD patterns for $La_{0.5}Sr_{0.5}CoO_3$ cathode powder as synthesized by different methods.

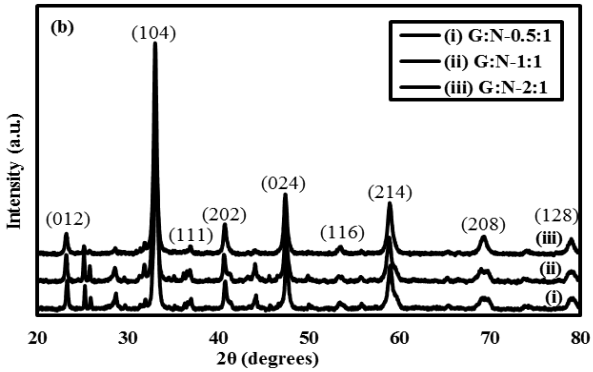

Fig. 3. (b) XRD patterns for $La_{0.5}Sr_{0.5}CoO_3$ cathode powder of different glycine and nitrate ratio as synthesized by glycine nitrate method.

Fig. 4 (a-c) shows morphology and EDX analyses of the LSCO powder as synthesized by different methods. The particle sizes are in micron range (approx. 0.5 µm) and well connected. From **Fig. 4 (a)** it is observed that particles of LSCO synthesized by so-gel method are agglomerated. It has been reported that substitution of Sr in $LaCoO_3$ structure increases the agglomeration [23]. The average particle size for LSCO powder synthesized by glycine-nitrate method and solid state route are between 0.5-1 µm and they are well connected to each other **(Fig. 4 (b), (c)).**

(a)

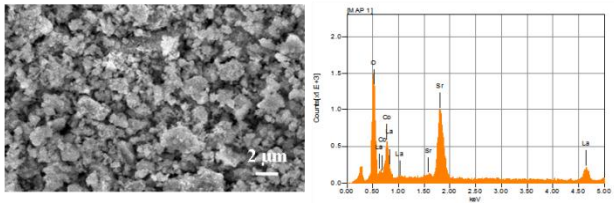

Fig. 4. (a) SEM image and EDX analysis of LSCO powder synthesized by sol-gel method after calcination at 850 °C for 10 h.

(b)

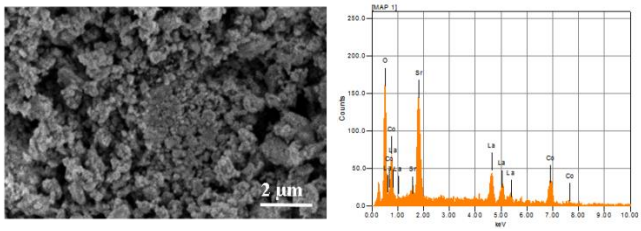

Fig. 4. (b) SEM image and EDX analysis of LSCO powder synthesized by glycine nitrate method after calcination at 850 °C for 10 h.

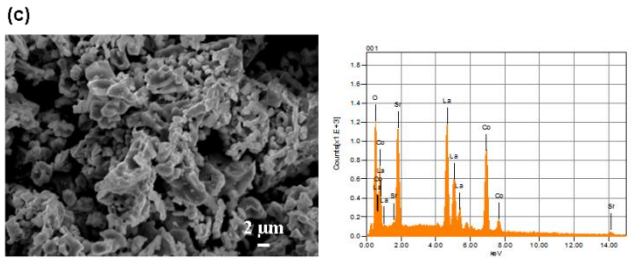

Fig. 4. (c) SEM image and EDX analysis of LSCO powder prepared by solid state route after sintering at 1250 °C for 12 h.

Slightly larger particle size has been observed for LSCO powder synthesized by solid state route due to high sintering temperature at 1250 °C. Presence of constituent elements La, Sr and Co in LSCO cathode is confirmed by EDX analysis.

Fig. 5 (a-c) show TEM micrographs of LSCO powder synthesized by different methods. It can be observed from TEM that the particle size (264 nm) of LSCO synthesized by glycine nitrate method is lesser than the particle size of cathode synthesized by sol-gel method (412 nm) and solid state route (797 nm). Large particle size and agglomeration in case of LSCO synthesized bysolid state route is due to high temperature treatment (1250 °C) in order to get perovskite phase. The LSCO pellets sintered at 1250 °C are investigated to assess phase purity and crystallite size of the samples using XRD analysis.

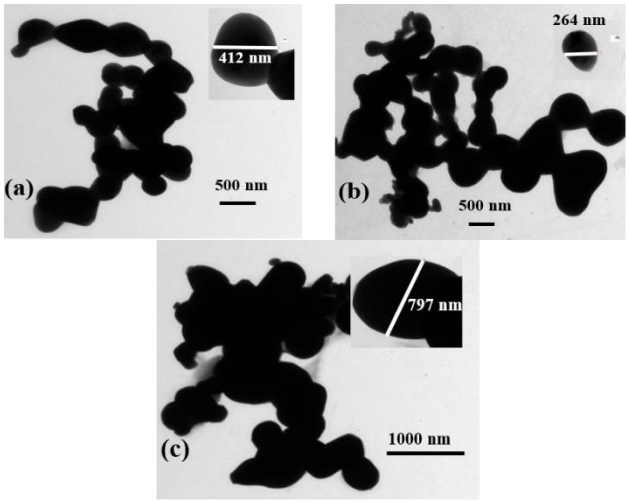

Fig. 5. TEM images of LSCO cathode material as synthesized by (a) sol-gel method, (b) glycine-nitrate method, and (c) solid state route.

Fig. 6 shows the XRD patterns of LSCO pellets. The observed major peaks of cathode pellets are matched with JCPDS card no. 48-0122 and confirms the formation of perovskite phase of LSCO. Some small peaks correspond to strontium oxide (JCPDS card no. 49-0692) at 48º and cobalt oxide (JCPDS Card No. 43-1004) at 61º have been also detected. Average crystallite size for LSCO cathode synthesized by different methods have been presented in **Table 2**. It is observed that smallest crystallite size (29.6 nm) has been observed for LSCO cathode synthesized by glycine nitrate method.

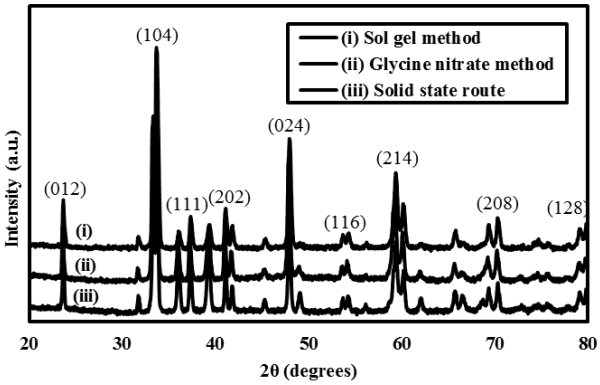

Fig. 6. XRD patterns for $La_{0.5}Sr_{0.5}CoO_3$ cathode sintered pellets as synthesized by different methods.

Table 2. Crystallite size of sintered pellets as synthesized by different methods.

Method	Crystallite Size (nm)
Sol gel method	32.2
Glycine nitrate method	29.6
Solid state route	37.1

Fig. 7 (a-c) show morphology, EDX analysis and elemental mapping of sintered LSCO cathode pellet synthesized by sol-gel method. It can be observed from SEM **(Fig. 7 (a))** that sufficient porosity is present such that high triple phase boundary is achieved. Particles are well connected and have stable structure. The presence of constituent elements are confirmed by EDX **(Fig. 7 (b)).** The homogenous distribution of constituent element can be seen in elemental mapping presented in **Fig. 7 (c).**

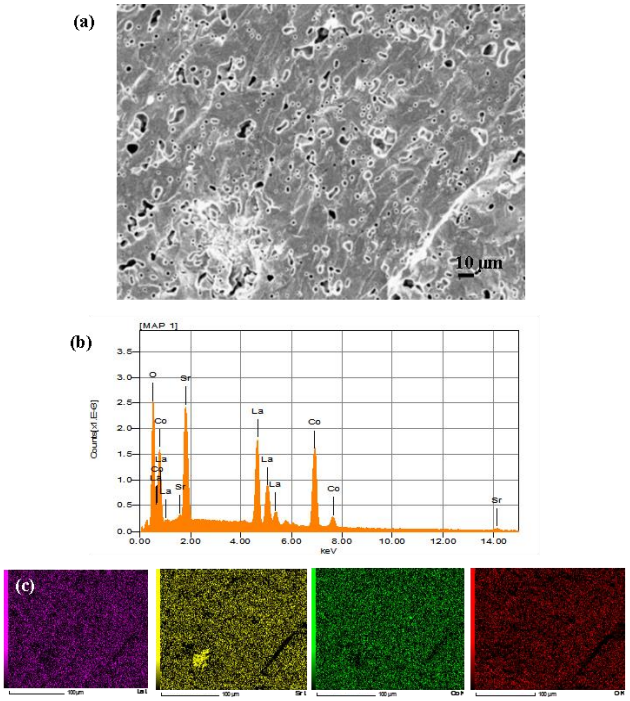

Fig. 7. (a) SEM image, (b) EDX analysis, and (c) Elemental mapping analysis of LSCO pellet by sol-gel method after sintering at 1250 °C for 12 h.

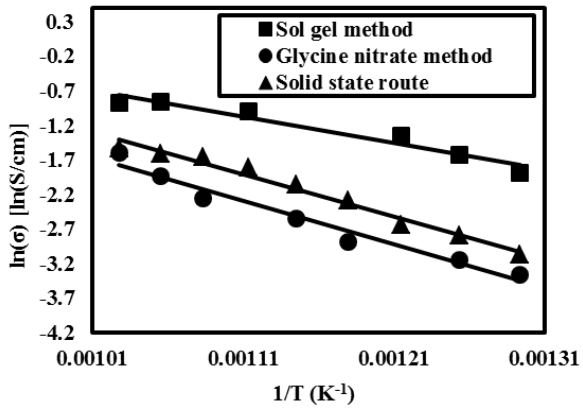

Fig. 8. Arrhenius plot for ionic conductivity of LSCO cathode material synthesized by different methods.

Fast oxygen ion transportation is essential for cathode materials hence ionic conductivity measurements has been done between 400-800 °C for the performance assessment of the LSCO cathode pellets in air atmosphere. **Fig. 8** shows Arrhenius plot for LSCO cathode material as synthesized by sol-gel, glycine-nitrate and solid state routes. The ionic conductivity for LSCO by sol-gel method initially increases with increase in temperature up to 700 °C then it remains constant till 800 °C. The highest ionic conductivity is 0.42 S/cm at 700 °C is observed for LSCO synthesized by sol-gel method. The ionic conductivity of LSCO synthesized by glycine-nitrate method and solid state route is found to be 0.20 S/cm and 0.22 S/cm at 700 °C. Endo et al. (2000) observed ionic conductivity of 0.1 S/cm for $La_{0.6}Sr_{0.4}CoO_3$ synthesized by Laser ablation method [20]. Ullmann et al. (2000) reported ionic conductivity of 0.22 S/cm at 800 °C for $La_{0.5}Sr_{0.5}CoO_{3-x}$ synthesized by spray drying [24], which is comparable to the ionic conductivity reported here even at lower temperature (700 °C). Lowest activation energy of 31.60 kJ/mol for LSCO synthesized by sol gel method has been observed between temperature range 500 to 700 °C. Activation energy for LSCO synthesized by glycine-nitrate method and solid state route is observed to be 52.48 kJ/mol and 51.28 kJ/mol, respectively. Egger et. al. (2012) reported activation energy of 118 kJ/mol at 725 °C for $La_{0.5}Sr_{0.5}CoO_{3-\delta}$ by modified Pechini process [14], which is much higher than what we observed. It is infer from above experimental results that LSCO cathode synthesized by sol-gel method has great potential for low/intermediate temperature solid oxide fuel cells due to its low activation energy.

To assess the performance of LSCO cathode, half-cell (LSCO/YDC) testing has been carried out between temperature 400-800 ºC. Area specific resistance (ASR) for the half cells has been calculated by impedance analysis at different temperature intervals. ASR provides the polarization losses corresponding to LSCO cathode. **Fig. 9 (a)** shows variation of ASR with temperature for half-cell having LSCO cathode as synthesized by different methods. As temperature increases ASR decreases which signifies lower polarization losses at higher temperature. Half-cell consists LSCO cathode synthesized by sol-gel method and YDC electrolyte shows reduction in ASR value from 6.44 Ω cm^2 at 700 °C to 3.52 Ω cm^2 at 800 °C. Half-cell consists LSCO cathode synthesized by glycine-nitrate method and YDC electrolyte shows reduction in ASR value from 18.30 Ω cm^2 at 700 °C to 11.26 Ω cm^2 at 800 °C but it is much higher than the LSCO synthesized by sol-gel method.

Half-cell consists LSCO cathode synthesized by solid state route and YDC electrolyte shows reduction in ASR value from 22.53 Ω cm^2 at 700 °C to 3.90 Ω cm^2 at 800 °C but higher than the LSCO synthesized by sol-gel method. Fracture surface of half-cell in **Fig. 9 (b)** shows 100 and 20 μm thick electrolyte and cathode respectively. YDC electrolyte is perfectly dense and shows proper adherence with cathode. There is no delamination or crack observed even after cell operation.

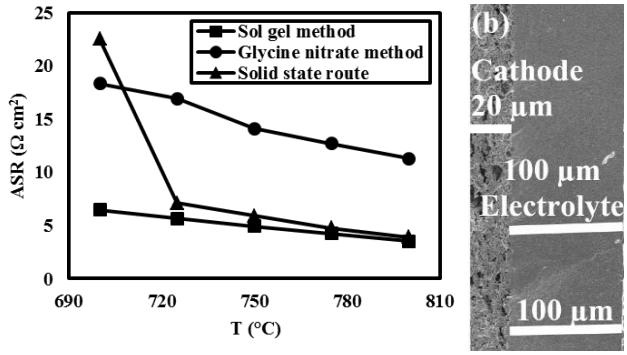

Fig. 9. (a) ASR variation with temperature for half-cell, and (b) SEM images of fracture surface of half-cell.

Fig. 10 (a-c) shows SEM images of different cathode pellets after operation. It is observed that cathode pellets synthesized by glycine nitrate method have lesser porosity than the other two methods. It can be infer that higher ASR value for half-cell having cathode synthesized by glycine nitrate is due to less porosity which hinder the oxygen movement.

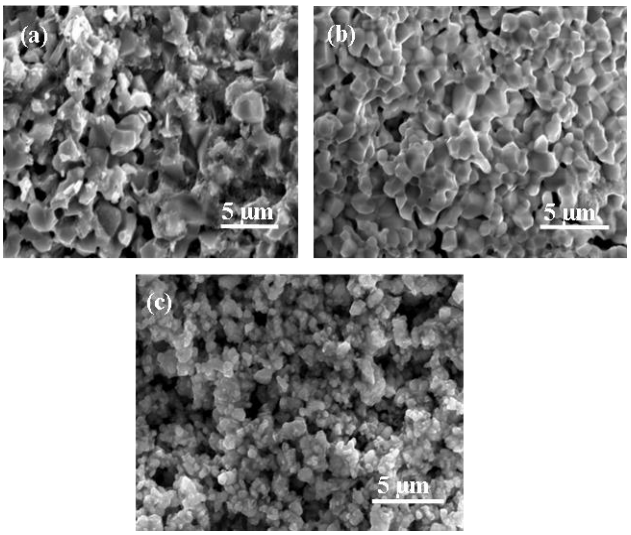

Fig. 10. SEM images of sintered LSCO pellet after operation synthesized by (a) sol-gel method, (b) glycine nitrate method, and (c) solid state route.

Conclusion

LSCO cathode material has been synthesized by three different methods i.e., sol-gel method, glycine-nitrate method and solid state route. Physical and electrical characteristics of LSCO has been compared in the present work. XRD confirms the formation of perovskite phase corresponds to LSCO. Smallest crystallite size of 21.9 nm has been observed for LSCO synthesized by glycine nitrate method (g/n=2:1). SEM and TEM of as synthesized cathode powder show well dispersed particles. Highest ionic conductivity, 0.42 S/cm at 700°C and activation energy, 31.60 kJ/mol between 500 to 700°C is exhibited by LSCO synthesized using sol-gel method. Sufficient porosity and uniform distribution of constituents has been observed in LSCO cathode matrix. The compatibility between YDC and LSCO even after co-sintering at 1250 °C shows their potential application for SOFC components at elevated temperature. Half-cell having LSCO cathode synthesized by sol-gel method shows lowest ASR, 3.52 Ω cm^2 at 800 °C.

References

1. Sun, C.; Hui, R.; Roller, J.; *J. Solid State Electrochem.*, **2010**, *14*, *1125*.
DOI: 10.1007/s10008-009-0932-0
2. Liu, B.; Liu, G.; Feng, H.; Wang, C.; Yang, H.; Wang, Y.; *Mater. Des.*, **2016**, *89*, *715*.
DOI: 10.1016/j.matdes.2015.10.034
3. Fu, Y.; Subardi, A.; Hsieh, M.; Chang, W.; *J. Am. Ceram. Soc.*, **2016**, *99*, *1345*.
DOI: 10.1111/jace.14127
4. Adler, S. B.; *Chem. Rev.*, **2004**, *104*, *4791*.
DOI: 10.1021/cr020724o
5. Jiang, S. P.; *J. Mater. Sci.*, **2008**, *43*, *6799*.
DOI: 10.1007/s10853-008-2966-6
6. Pelosato, R.; Cordaro, G.; Stucchi, D.; Cristiani, C.; Dotelli, G.; *J. Power Sources*, **2015**, *298*, *46*.
DOI: 10.1016/j.jpowsour.2015.08.034
7. Gomez, A. M.; Sacanell, J.; Leyva, A. G.; Lamas, D. G.; *Ceram. Int.*, **2016**, *42*, *3145*.
DOI: 10.1016/j.ceramint.2015.10.104
8. Park, J. S.; Kim, Y. B.; *Thin Solid Films*, **2016**, *599*, *174*.
DOI: 10.1016/j.tsf.2015.12.042
9. Burye, T. E.; Nicholas, J. D.; *J. Power Sources*, **2015**, *276*, *54*.
DOI: 10.1016/j.jpowsour.2014.11.082
10. Lopez, E. G.; Marci, G.; Puleo, F.; Parola, V. L.; Liotta, L. F.; *Appl. Catal., B*, **2015,** *178*, *218*.
DOI: 10.1016/j.apcatb.2014.09.014
11. Basu, S.; Recent Trends in Fuel Cell Science and Technology; Springer: USA, **2007**.
DOI: 10.1007/978-0-387-68815-2_3
12. Su, Q.; Gong, W.; Yoon, D.; Jacob, C.; Jia, Q.; Manthiram, A.; Jacobson, A. J.; Wang, H.; *J. Electrochem. Soc.*, **2014**, *161*, *F398*.
DOI: 10.1149/2.026404jes
13. Kima, E. H.; Jung, H. J.; An, K. S.; Park, J. Y.; Lee, J.; Hwang, D.; Kim, J. Y., Leed, M. J.; Kwona, Y.; Hwang, J. H.; *Ceram. Int.*, **2014**, *40*, *7817*.
DOI: 10.1016/j.ceramint.2013.12.125
14. Choudhury, P. R.; Parui, J.; Chiniwar, S.; Krupanidhi, S. B.; *Solid State Commun.*, **2015**, *208*, *15*.
DOI: 10.1016/j.ssc.2015.02.011
15. Egger, A.; Bucher, E.; Yang, M.; Sitte, W.; *Solid State Ionics*, **2012**, *225*, *55*.
DOI: 10.1016/j.ssi.2012.02.050
16. Lee , S.; Hu, Y.; *Surf. Coat. Technol.*, **2013**, *231*, *293*.
DOI: 10.1016/j.surfcoat.2012.02.028
17. Hu, Y.; Bouffanais, Y.; Almar, L.; Morata, A.; Tarancon, A.; Dezanneau, G.; *Int. J. Hydrogen Energy*, **2013**, *38*, *3064*.
DOI: 10.1016/j.ijhydene.2012.12.047
18. Ou, D. R.; Cheng, M.; *J. Power Sources*, **2014**, *272*, *513*.
DOI: 10.1016/j.jpowsour.2014.08.077
19. Endo, A.; Wada, S.; Wen, C.; Komlyama, H.; Yamada, K.; *J. Electrochem. Soc.*, **1998**, *145*, *L35*.
DOI: 10.1149/1.1838332
20. Endo, A.; Fukunaga, H.; Wen, C.; Yamada, K.; *Solid State Ionics*, **2000**, *135*, *353*.
DOI: 10.1016/S0167-2738(00)00466-5
21. Samat, A. A.; Ishak, M. A. M.; Hamid, H. A.; Osman, N., *Adv. Mater. Res.*, **2013**, *701*, *131*.
DOI: 10.4028/www.scientific.net/AMR.701.131
22. Tao, Y.; Shao, J.; Wang, J.; Wang, W. G.; *J. Power Sources*, **2008**, *185*, *609*.
DOI: 10.1016/j.jpowsour.2008.09.021
23. Lal, B.; Raghunandan, M. K.; Gupta, M.; Singh, R. N.; *Int. J. Hydrogen Energy*, **2005**, *30*, *723*.
DOI:10.1016/j.ijhydene.2004.07.002
24. Ullmann, H.; Trofimenko, N.; Tietz, F.; Stover, D.; Ahmad-Khanlou, A.; *Solid State Ionics*, **2000**, *138*, *79*.
DOI: 10.1016/S0167-2738(00)00770-0

